Independently Tunable Multichannel Fractional-Order Temporal Differentiator Based on a Silicon-Photonic Symmetric Mach–Zehnder Interferometer Incorporating Cascaded Microring Resonators

Weifeng Zhang, *Student Member, IEEE*, Weilin Liu, *Student Member, IEEE*, Wangzhe Li, *Student Member, IEEE*, Hiva Shahoei, *Student Member, IEEE*, and Jianping Yao, *Fellow, IEEE, Fellow, OSA*

***Abstract*—A multichannel fractional-order temporal differentiator with independently tunable differentiation order based on an integrated silicon-photonic symmetric Mach–Zehnder interferometer consisting of cascaded microring resonators (MRRs) is designed, fabricated, and experimentally demonstrated. By controlling the radii of the MRRs, a multichannel spectral response with uniform channel spacing is obtained, which is used to function as a multichannel temporal differentiator with multiple subdifferentiators. The differentiation order of each subdifferentiator is independently tunable by optically pumping the corresponding MRR, which leads to the phase change in the spectral response due to the two-photon absorption induced nonlinear effect. A five-channel temporal differentiator with a channel spacing of 0.49 nm is fabricated on a silicon-on-insulator chip using a CMOS-compatible process with 193-nm-deep ultraviolet lithography. Independent tuning of the differentiation orders of the subdifferentiators is experimentally demonstrated.**

***Index Terms*—Analog optical signal processing, micro-ring resonators, microwave photonics, silicon photonics, temporal differentiator.**

I. Introduction

A photonic temporal differentiator, performing temporal differentiation of the complex envelope of an arbitrary optical signal, is one of the basic signal processing blocks, which can find numerous applications such as in ultrafast computing [1], ultra-short pulse generation [2], [3] and ultra-short pulse characterization [4]. In general, a photonic temporal differentiator can be realized using an optical device that has a transfer function given by $[j(\omega - \omega_0)]^n$, where n is the differentiation order, ω is the optical frequency and ω_0 is the optical carrier frequency. When the differentiation order n is not 1, the operator is generalized to be a fractional-order photonic temporal differentiator [5], [6].

Due to the inherent advantages such as much higher speed and wider bandwidth offered by photonics, a temporal differentiator implemented in the optical domain can perform ultra-high speed and wideband operation, which is not achievable by the electronic counterpart. Different schemes have been proposed, which include fiber-based and silicon-based solutions. For example, an all-optical temporal differentiator could be implemented using a phase-shifted fiber Bragg grating (PS-FBG) [7], a silicon-based micro-ring resonator (MRR) [8] and a silicon-based phase-shifted waveguide Bragg grating (PS-WBG) [9]. A temporal differentiator based on a PS-FBG is relatively easy to implement, but it is highly sensitive to environmental changes. A silicon-based differentiator based on an MRR or a PS-WBG has the advantages of small footprint and can be integrated with other optical and electronic devices. However, the differentiation order of the temporal differentiators in [7]–[9] is 1, which is fixed and not tunable. Due to the potential applications in pulse shaping, signal processing and ultrafast optical signal coding, a temporal differentiator with a tunable fractional order is important. In [5], a photonic fractional-order temporal differentiator implemented based on an asymmetrical PS-FBG in reflection was demonstrated. The limitation of this technique is again the absence of the differentiation order tunability. Recently, the implementation of a fractional differentiator using a titled fiber Bragg grating (TFBG) was demonstrated [10]. In a TFBG, the phase response at a cladding mode resonant wavelength is strongly polarization dependent. By continuously tuning the polarization state of the input light wave, the fractional order is continuously tuned. Based on the same principle, a tunable fractional-order temporal differentiator using a polarization-dependent silicon-based MRR incorporating a multimode interference coupler was experimentally demonstrated [11]. However, the change of the polarization state usually involves mechanical movement, making the system complicated with low accuracy.

With the fast growth of information exchange all over the world, wavelength-division multiplexing (WDM), as a promising technology for expanding the capacity for optical

Manuscript received August 9, 2014; revised October 24, 2014; accepted December 1, 2014. Date of publication December 3, 2014; date of current version January 23, 2015. This work was supported in part by the Natural Science and Engineering Research Council of Canada through the CREATE Program and the CMC Microsystems.

The authors are with the Microwave Photonics Research Laboratory, School of Electrical Engineering and Computer Science, University of Ottawa, Ottawa ON K1N6N5, Canada (e-mail: jpyao@eecs.uOttawa.ca).

Color versions of one or more of the figures in this paper are available online at http://ieeexplore.ieee.org.

Digital Object Identifier 10.1109/JLT.2014.2377657

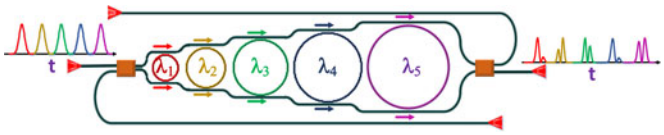

Fig. 1. Schematic layout of the proposed multi-channel fractional-order temporal differentiator.

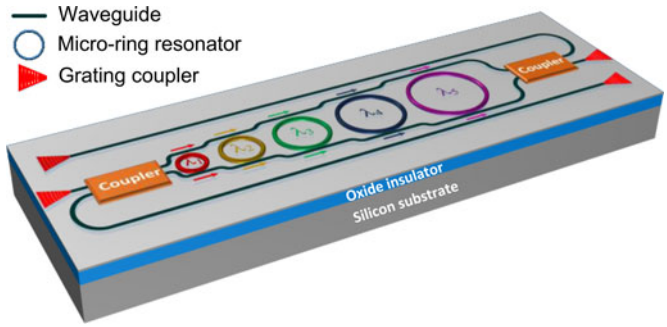

Fig. 2. Perspective view of the proposed multi-channel fractional-order temporal differentiator.

communications, has been widely used in the present optical communications networks [12]. For ultrafast signal processing and characterization in a WDM network, an all-optical temporal differentiator that is capable of performing temporal differentiation of multichannel signals carried by multiple wavelengths is required. However, in the above-mentioned fiber-based temporal differentiators, the channel number is always one. A multi-channel optical differentiator can be implemented based on an optical interferometer. The response of an interferometer is intrinsically periodic in frequency. This fact has been exploited for the measurement and characterization of multi-wavelength high-speed signals in a WDM communications system [13]. The main limitation of this solution is the poor stability due to the high sensitivity of an interferometer to environmental fluctuations. Another solution is to use a single multi-channel fiber Bragg grating (MC-FBG) [14]. A MC-FBG can be designed using the discrete layer peeling algorithm together with the spatial sampling technique. However, in the both techniques [13], [14], once the device is fabricated, the differentiation order is fixed.

A multi-channel optical differentiator can also be implemented based on a silicon-based MRR. Again, thanks to the periodic response of the MRR, it is possible to use integrated device for multi-channel signal processing. However, the free spectral range (FSR) of an MRR is usually much larger than the channel spacing of a WDM communications system, or if an MRR is designed to meet the channel spacing of a WDM communications system, the radius will be very large and the chip footprint is significantly increased. In this paper, we report, to the best of our knowledge, the first demonstration of an independently tunable multi-channel fractional-order temporal differentiator implemented based on silicon-photonic MRR. The proposed tunable multi-channel fractional-order temporal differentiator has a symmetric Mach–Zehnder interferometer (MZI) structure, in which multiple MRRs are cascaded. By carefully designing the radii of the multiple MRRs and the couplers, a multi-channel spectral response with identical channel spacing is obtained, which is used to implement a multi-channel fractional-order temporal differentiator. When a pump light is fed into an MRR, the phase response of the MRR is changed by tuning the power of the pump light thanks to the two-photon absorption (TPA) induced nonlinear effect in the MRR. Thus, the order of the temporal differentiator is tuned. A five-channel temporal differentiator is fabricated on a silicon-on-insulator chip using a CMOS-compatible process with 193 nm deep ultraviolet lithography. Spectral measurement shows a five-channel response with a channel spacing of 0.49 nm and a bandwidth of each channel of 0.032 nm. The tunability of the differentiation order of a specific channel is realized by locating the pumping wavelength at a resonant wavelength of the specific MRR and by tuning the power of the pumping light. The key feature of the proposed multi-channel temporal differentiator is that WDM signals at multiple optical wavelengths can be simultaneously differentiated and the fractional order of each individual channel can be independently tuned, which gives more flexibility for ultra-fast signal processing in WDM systems.

II. Design and Measurement

Fig. 1 illustrates the layout of the proposed multi-channel fractional-order temporal differentiator. It has a symmetric MZI structure incorporating multiple cascaded MRRs. The MZI comprises two adiabatic 3-dB couplers [15]. To minimize the chip footprint and to reduce the bending loss, a strip waveguide structure is used to guide the light in the chip. Grating couplers [16] are employed to couple the light into or out of the chip. The input light is split by the first adiabatic 3-dB coupler into two beams to travel through the upper and lower arms. Each ring will selectively transfer the optical power at its resonance wavelength from the through-port waveguide to its drop-port waveguide. The MRRs in Fig. 1 are shown in different colors, to indicate that each MRR is designed to have a different radius and therefore a different resonant wavelength. The spacing between the neighbor MRRs is large enough to avoid mutual interferences. In the upper and lower waveguides, S-shape waveguide bends, which are designed using Bezier curves to minimize the mode mismatch and thus reduce the waveguide bending loss [17], are added to adapt to the change of the rings. The wavelengths from the two waveguides will be recombined at the second adiabatic 3-dB coupler at the transmission port. By carefully designing the ring radii, at the transmission port, the multi-channel response with identical channel spacing within the expected bandwidth can be achieved. Thus, a multi-channel temporal differentiator can be implemented. Fig. 2 shows the perspective view of the proposed multi-channel fractional-order temporal differentiator. Note that in Fig. 1, for measurement convenience, the reflection port has its independent grating coupler. One key advantage of the proposed structure is the reconfigurability of the design. The MRRs are designed to have different radii that are adapted by the two specially designed MZI arms, which give the convenience to expand to incorporate more rings. The multi-channel

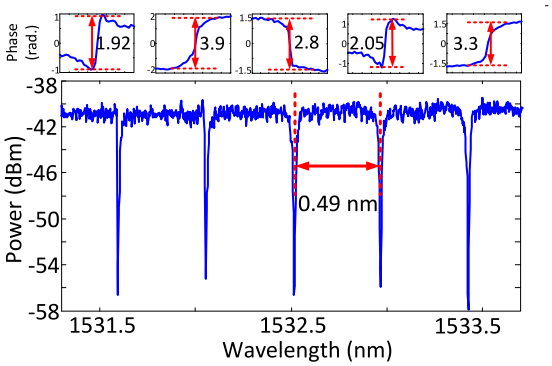

Fig. 3. Measured spectral response of the five-channel fractional-order temporal differentiator; Inset: measured phase response of the five-channel fractional-order temporal differentiator.

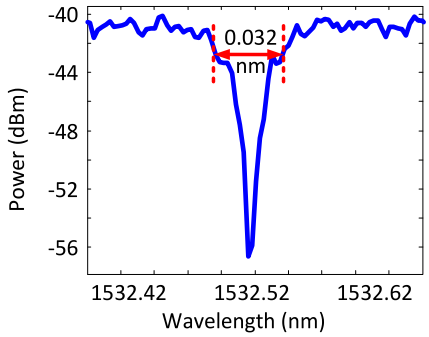

Fig. 4. Zoom-in view of spectral response of the third channel of the five-channel fractional-order temporal differentiator.

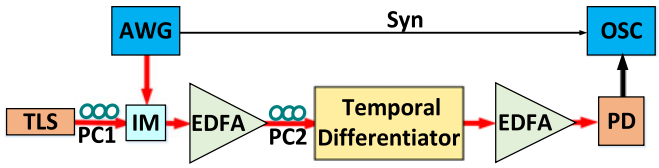

Fig. 5. Experimental setup. TLS: Tunable laser source. IM: Intensity modulator. AWG: Arbitrary waveform generator. EDFA: Erbium-doped fiber amplifier. PC: Polarization controller. PD: Photodetector. OSC: Oscilloscope.

temporal differentiator based on this design has smaller size with better compactness, especially the drop port can share a common port with the input port.

The proposed structure can also be employed as a spectral shaper with an arbitrary spectral response. A spectral shaper with a reconfigurable spectral response is useful for the implementation of an all-optical microwave arbitrary waveform generator (AWG) to generate arbitrary microwave waveforms such as a chirped waveform, which was recently demonstrated by us [18].

The designed device is fabricated using a CMOS-compatible technology with 193-nm optical projection lithography at IMEC, Belgium, accessed via ePIXfab. The waveguide consists of a thin silicon layer (220 nm thick) on top of a buried oxide layer (2 μm thick) on a silicon wafer. The strip waveguide is employed as the fundamental waveguide structure. In order to support single transverse-electric mode propagation, the strip waveguide width is chosen to be 500 nm. The radii of the five MRR are designed to be 20.452, 20.964, 21.476, 21.990 and 22.506 μm so that the multi-channel response with identical channel spacing within the expected bandwidth is achieved. The coupling gaps between the MRRs and the two arms of the MZI are kept identical. Due to the propagation loss in the MRRs, the five add-drop MRRs would operate in the undercoupling regime [19]. The entire device is 1.175 mm in length and 0.063 mm in width, giving a small footprint of 0.074 mm^2. The footprint of the device can still be greatly decreased if a compact Y-branch [20] is used to replace the adiabatic 3-dB coupler.

The spectral and phase responses are measured using an optical vector analyzer (LUNA OVA CTe). Fig. 3(a) shows the spectral response of the five-channel fractional-order temporal differentiator with a channel spacing of 0.49 nm measured at the transmission port. The phase response for each of the five channels is also shown in Fig. 3 as an insert. The FSRs of the MRR are 4.383, 4.275, 4.154, 4.094 and 4.060 nm. Fig. 4 shows the zoom-in view of the spectral response for the third channel, which shows that the channel has a bandwidth of 0.032 nm or 4 GHz. Such a channel can be used for the implementation of an optical differentiator with an operation bandwidth of 4 GHz. Based on the spectral response in Fig. 4, we can estimate the Q-factor of the MRR, which is about 4×10^5. A high Q-factor ensures an MRR to have strong capacity in light confinement, which enables relatively low power pumping of the MRR to introduce the required phase response change. On the other hand, a high Q-factor makes an MRR to have a relatively small bandwidth. Thus, there is a trade-off between the operation bandwidth and the required pumping power.

III. Principle and Experiment

For an input signal $x(t)$, the Fourier transform of its n-th order differentiation, $dx^n(t)/dt^n$, is expressed as $[j(\omega - \omega_0)]^n X(\omega - \omega_0)$, where ω is the optical frequency, ω_0 is the carrier frequency, and $X(\omega)$ is the Fourier transform of $x(t)$. Therefore, the differentiator can be considered as an optical filter with a frequency response given by

$$H(\omega) = [j(\omega - \omega_0)]^n = \begin{cases} e^{jn\left(\frac{\pi}{2}\right)} |\omega - \omega_0|^n, & \omega > \omega_0 \\ e^{jn\left(-\frac{\pi}{2}\right)} |\omega - \omega_0|^n, & \omega < \omega_0 \end{cases}. \quad (1)$$

As can be seen an nth-order temporal differentiator can be implemented using an optical filter that has a magnitude response of $|\omega - \omega_0|^n$ and a phase jump of θ at ω_0, where $\theta = n\pi$. When θ is not multiple times of π, the differentiation order is generalized to be a fractional-order with $n = \theta/\pi$. When the phase jump is tuned, the differentiation order is tuned.

To verify that the fabricated device can be used to implement a multi-channel temporal differentiator with independently tunable differentiation order, an experiment is carried out. The experimental setup is shown in Fig. 5. A continuous-wave light wave from a tunable laser source (TLS) is directed to an intensity modulator (IM) via a polarization controller (PC1). An

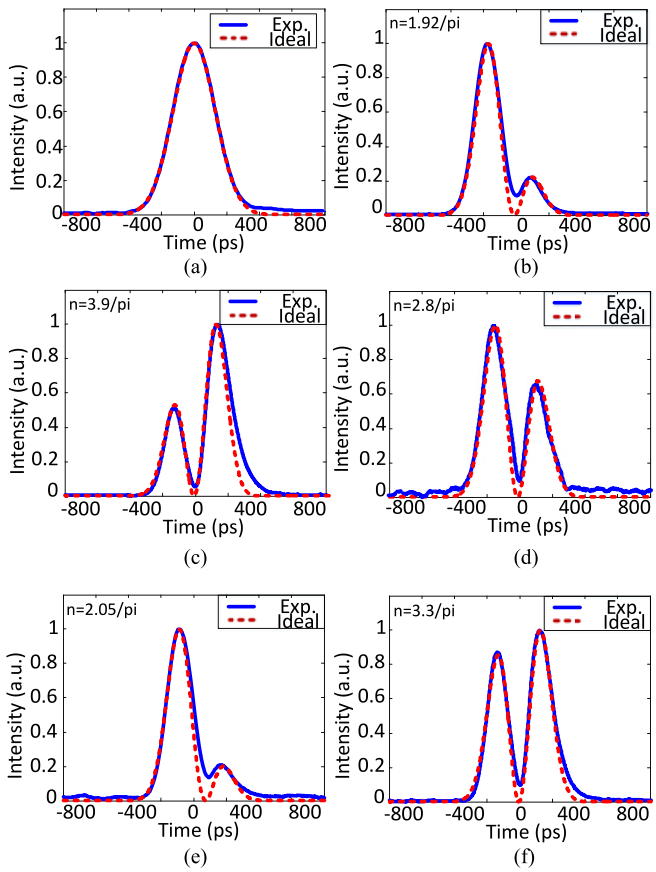

Fig. 6. Experimental results. (a) The measured Gaussian pulse from AWG (the blue solid line) and the simulated Gaussian pulse (the red dotted line); and measured differentiated output pulses from the photonic fractional differentiator at the (b) first, (c) second, (d) third, (e) fourth, and (f) fifth channel.

electrical pulse from an AWG (Tektronix AWG7102) is applied to modulate the optical carrier at the IM. The pulse from the AWG has a shape close to a Gaussian with a temporal full-width at half-maximum of about 360 ps, or a spectral width of about 4 GHz, as shown in Fig. 6(a). The optical signal is then sent to the chip through a second polarization controller (PC2) which adjusts the state of polarization of the input light wave to minimize the polarization-dependent loss. Since the central portion of the input signal spectrum is filtered out in the differentiator, the temporal differentiation is an operation with an inherently low energetic efficiency. To compensate for the loss, the optical signal is amplified before and after the temporal differentiator using two erbium-doped fiber amplifiers (EDFAs). Finally, the output optical pulse is detected by a high-speed photodetector (PD) with the waveform observed by a high-speed sampling oscilloscope (OSC, Agilent 86116A).

Fig. 6 shows the measured temporally differentiated pulses at the output of the five-channel fractional-order temporal differentiator for five optical wavelengths of 1531.564, 1532.006, 1532.460, 1532.948 and 1533.438 nm, for an input Gaussian pulse from the AWG, shown in Fig. 6(a) (blue-solid line). A simulated Gaussian pulse (red-dashed line) is also shown in Fig. 6(a) for comparison. Fig. 6(b) shows the corresponding temporally differentiated pulse (blue-solid line) by the first channel with a

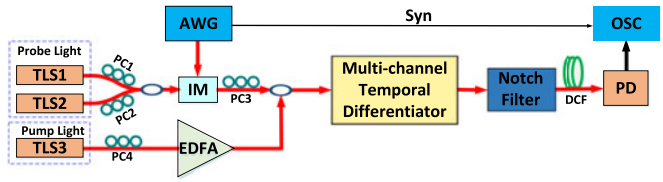

Fig. 7. Experimental setup. TLS: Tunable laser source. IM: Intensity modulator. AWG: Arbitrary waveform generator. EDFA: Erbium-doped fiber amplifier. PC: Polarization controller. PD: Photodetector. OSC: Oscilloscope. DCF: Dispersion compensating fiber.

differentiation fraction order of 0.61. Again, a simulated temporally differentiated pulse (red-dashed line) is also shown for comparison. As can be seen the experimentally generated pulse is close to the simulated pulse, which confirms the effectiveness of the use of the device to perform fractional-order differentiation. Fig. 6(c)–(f) shows the temporally differentiated pulses by the other four channels, with differentiation orders of 1.24, 0.89, 0.65 and 1.05. Again, good agreement is achieved, which confirms again the effectiveness of the use of the device to perform a fractional-order differentiation. Thus, the multi-channel operation of the fractional-order temporal differentiator has been demonstrated. The root mean square errors (RMSEs) of the five differentiators with fractional orders of 0.61, 1.24, 0.89, 0.65 and 1.05 are calculated, which are 2.0%, 3.4%, 3.2%, 2.2% and 3.2%, respectively

IV. Independent Tunability

We then demonstrate the independent differentiation order tunability. The experimental setup is shown in Fig. 7. The difference between the setup in Fig. 7 and that in Fig. 5 is that a wavelength-tunable light source is used as a pumping light to perform the differentiation order tuning.

We first demonstrate the differentiation order tuning. In this case, only a single probe signal is applied to the chip. A pumping light is amplified by a high power EDFA (Amonics, AEDFA-33-B-FA) and sent to the chip together with the probe light via a coupler. The wavelength of the pumping light is selected different from the wavelength of the probe light, but is located at one resonant wavelength of the MRR to increase the light confinement, thus with increased nonlinear optical effect. At the output of the chip, a notch filter is used to remove the pumping light to avoid possible damage to the PD. The differentiated pulse is detected by the PD and the waveform is observed by the OSC. Thanks to the nonlinear thermo-optic effect in the silicon-based MRR, when the pumping light at a different power level is fed into the MRR, the phase response of the MRR is changed [21]–[23]. The strong light-confinement nature of the MRR makes the MRR have a strong response to the nonlinear optical effect. Thus, the tuning is achieved at a low pumping power level. As it was demonstrated in [24], for the implementation of a temporal differentiator, the phase response is more important than the magnitude response. The magnitude response of an ideal temporal differentiator is given by $|\omega - \omega_0|^n$, which may not be exactly satisfied by using an MRR. The phase jump provided

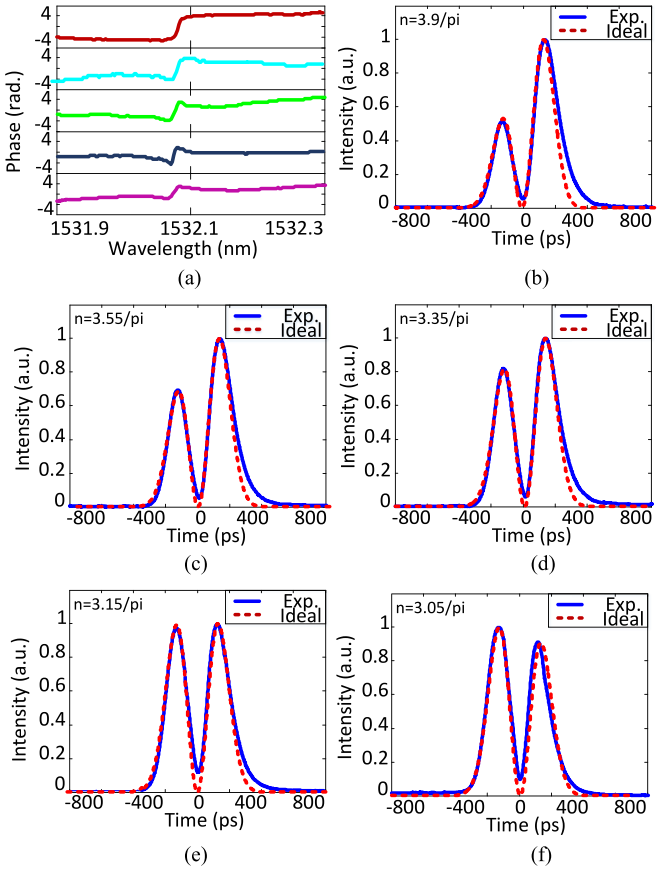

Fig. 8. Experimental results for differentiation order tuning. (a) Measured phase response of the second channel with the power of the pump light increased, and measured differentiated output pulses from the photonic fractional differentiator at the second channel with the pump light wave power of (b) 0, (c) 21.7, (d) 25, (e) 28.7, and (f) 31 dBm.

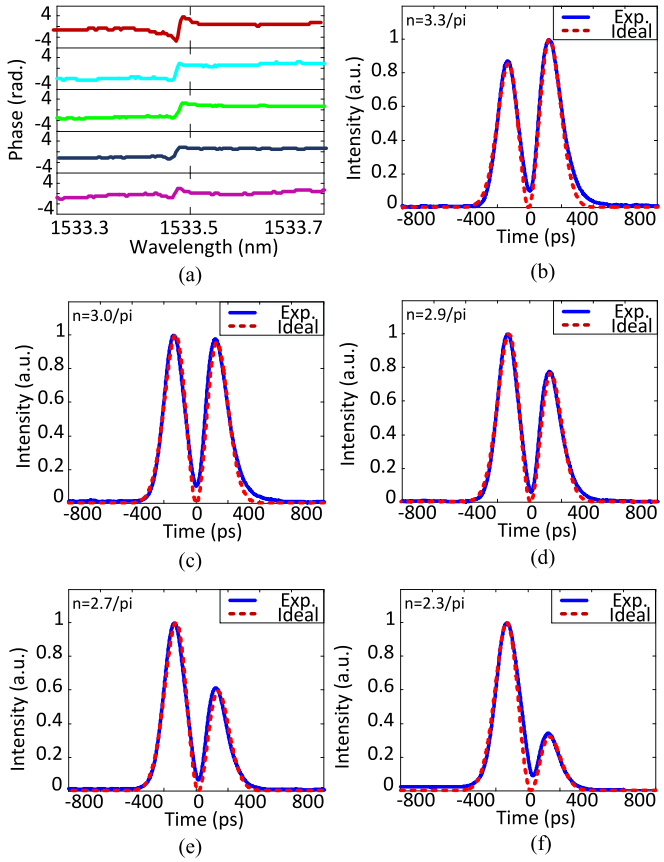

Fig. 9. Experimental results for differentiation order tuning: (a) Measured phase response of the second channel with the power of the pumping light increased, and the measured differentiated output pulses from the differentiator at the fifth channel with the pumping power at (b) 0, (c) 21.7, (d) 25, (e) 28.7, and (f) 31 dBm.

by an MRR is critical for the implementation of a temporal differentiator. When the phase jump is tuned by tuning the power of the pump light, a temporal differentiator with a tunable differentiation order is achieved.

Fig. 8 shows the measured differentiated pulses at the output of the second channel for a probe light at 1532.006 nm and a pumping light at 1536.280 nm. The pump light wavelength is selected at one resonance wavelength of the second MRR. Fig. 8(a) shows the measured phase response of the second channel with the pumping power increased from 0 to 31 dBm. As can be seen, with the increase of the pump power, the phase jump becomes smaller, which is resulted from the increase in the internal loss in the MRR due to the TPA-induced nonlinear effect. Fig. 8(b)–(f) shows the corresponding temporally differentiated pulse (blue-solid line). Differentiated pulses with differentiation orders of 1.24, 1.13, 1.07, 1.00, and 0.97 are generated. The simulated pulses with an ideal input Gaussian pulse and an ideal differentiator with the same orders are also shown (red-dashed line) for comparison. As can be seen the experimentally generated pulses are close to the simulated pulses, which confirms the effectiveness of the use of the device to perform a tunable fractional-order differentiator. The RMSEs of the differentiators with fractional orders of 1.24, 1.13, 1.07, 1.00 and 0.97 are also calculated, which are 3.4%, 3.6%, 3.8%, 3.0% and 2.4%, respectively.

Fig. 9 shows the measured differentiated pulses at the output of the fifth channel for a probe light wavelength at 1533.438 nm and a pumping light wavelength at 1537.498 nm. The pumping light wavelength is selected at one resonance wavelength of the fifth MRR. Fig. 9(a) shows the measured phase response of the second channel with the pumping power increased from 0 to 31 dBm. Fig. 9(b)–(f) shows the corresponding temporally differentiated pulse (blue-solid line). Differentiated pulses with differentiation orders of 1.05, 0.96, 0.92, 0.86, and 0.73 are generated. The RMSEs of the differentiators with fractional orders of 1.05, 0.96, 0.92, 0.86 and 0.73 are again calculated, which are 3.2%, 3.2%, 2.6%, 2.2% and 2.1%, respectively. The experimental results in Figs. 8 and 9 confirm that the tuning of a sub-differentiator can be done by selecting the pumping wavelength.

Then, we verify that when one channel is pumped, the other channel is not affected. To do so, we send two probe light waves at two wavelengths at 1532.006 and 1533.438 nm corresponding to two resonant wavelengths of the second and the fifth channels. A dispersion compensating fiber (DCF) is added to the setup in Fig. 7 to temporally separate the outputs from the two channels

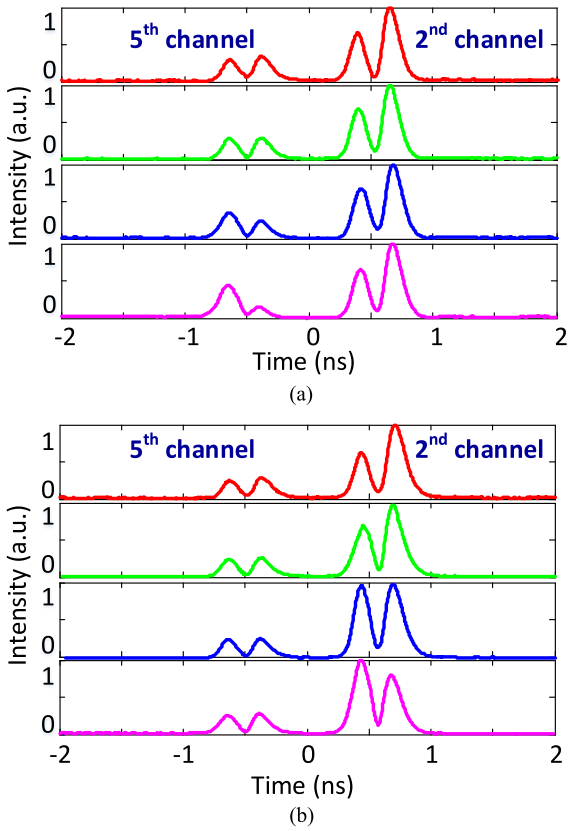

Fig. 10. Experimental results for independent tunability. Measured differentiated output pulses from the differentiator at the second and the fifth channels with the pumping light wavelength at (a) 1537.498 nm corresponding a resonant wavelength of the fifth channel, and (b) 1535.920 nm corresponding a resonant wavelength of the second channel.

due to the dispersion-induced time delay between the two probe lights, for the purpose of waveform observation.

First, the wavelength of the pumping light is selected at one resonance wavelength of the fifth MRR. Fig. 10(a) shows the measured differentiated pulses at the output of the differentiator. The pulses on the left correspond to the output from the fifth channel and on the right correspond to the output from the second channel. The magnitude difference between the differentiated pulses from the two channels is resulted from the different amplitude resonance of the two channels. When the pumping wavelength is selected at 1537.498 nm corresponding a resonant wavelength of the fifth channel and the pumping power is increased from 0 to 31 dBm, the order of the differentiated pulse at the output fifth channel is changed while the order of the differentiated pulse at the second channel is maintained unchanged. Second, the wavelength of the pumping light is selected at one resonance wavelength of the second MRR. When the pumping wavelength is selected at 1535.920 nm corresponding a resonant wavelength of the second channel and the pumping power is increased from 0 to 31 dBm, the order of the differentiated pulse at the output of the second channel is changed while the order of the differentiated pulse at the fifth channel is maintained unchanged. The experimental results in Fig. 10 confirm that the differentiation order of each sub-differentiator in the proposed integrated on-chip multi-channel differentiator is independently tuned.

V. Conclusion

An on-chip independently tunable multi-channel fractional-order temporal differentiator was designed, fabricated and experimentally demonstrated. The proposed differentiator has a symmetric MZI structure, in which multiple MRRs were cascaded. By controlling the radii of the MRRs, a multi-channel response with identical wavelength spacing was achieved. The differentiation order tuning of an MRR was achieved by optically pumping the MRR. Due to the nonlinear thermo-optic effect, the phase response of the MRR could be changed by tuning the power of the pumping light at one resonant wavelength of the MRR. A five-channel temporal differentiator was fabricated using a CMOS-compatible process with 193 nm deep ultraviolet lithography. Spectral measurement showed that the temporal differentiator had a spectra response with five channels with an identical channel spacing of 0.49 nm and each channel has a bandwidth of 0.032 nm. The use of the five-channel temporal differentiator to perform multi-channel differentiation with independently tunable differentiation order was demonstrated.

The key feature of the proposed temporal differentiator is that a WDM signal at multiple wavelengths can be simultaneously differentiated and the fractional order of each individual channel can be independently tuned, which gives much more flexibility in WDM signal processing.

Acknowledgment

This work was supported by the Natural Sciences and Engineering Research Council of Canada under the Silicon Electronic-Photonic Integrated Circuits CREATE program. The authors would also like to thank CMC Microsystems, for providing the design tools and enabling the fabrication of the device.

References

[1] J. Azaña, "Ultrafast analog all-optical signal processors based on fiber-grating devices," *IEEE Photon. J.*, vol. 2, no. 3, pp. 359–386, Jun. 2010.
[2] J. P. Yao, F. Zeng, and Q. Wang, "Photonic generation of ultra-wideband signals," *J. Lightw. Technol.*, vol. 25, no. 11, pp. 3219–3235, Dec. 2007.
[3] J. A. N. Da Silva and M. L. R. De Campos, "Spectrally efficient UWB pulse shaping with application in orthogonal PSM," *IEEE Trans. Commun.*, vol. 55, no. 2, pp. 313–322, Feb. 2007.
[4] F. Li, Y. Park, and J. Azaña, "Complete temporal pulse characterization based on phase reconstruction using optical ultrafast differentiation (PROUD)," *Opt. Lett.*, vol. 32, no. 22, pp. 3364–3366, Nov. 2007.
[5] C. Cuadrado-Laborde and M. V. Andrés, "In-fiber all-optical fractional differentiator," *Opt. Lett.*, vol. 34, no. 6, pp. 833–835, Mar. 2009.
[6] C. Cuadrado-Laborde, "All-optical ultrafast fractional differentiator," *Opt. Quantum Electron.*, vol. 40, no. 13, pp. 983–990, Mar. 2009.
[7] N. K. Berger, B. Levit, B. Fischer, M. Kulishov, D. V. Plant, and J. Azaña, "Temporal differentiation of optical signals using a phase-shifted fiber Bragg grating," *Opt. Exp.*, vol. 15, no. 2, pp. 371–381, Jan. 2007.
[8] F. Liu, T. Wang, L. Qiang, T. Y. Zhang, M. Qiu, and Y. Su, "Compact optical temporal differentiator based on silicon microring resonator," *Opt. Exp.*, vol. 16, no. 20, pp. 15880–15886, Sep. 2008.
[9] W. Zhang, W. Li, and J. P. Yao, "Optical differentiator based on an integrated sidewall phase-shifted Bragg grating," *IEEE Photon. Technol. Lett.*, vol. 26, no. 23, pp. 2383–2386, Dec. 2014.
[10] M. Li, L. Shao, J. Albert, and J. P. Yao, "Continuously tunable photonic fractional temporal differentiator based on tilted fiber Bragg grating," *IEEE Photon. Technol. Lett.*, vol. 23, no. 4, pp. 251–253, Feb. 2011.

[11] H. Shahoei, D. Xu, J. Schmid, and J. P. Yao, "Tunable photonic fractional-order differentiator by coupling tuning of an SOI microring resonator," *IEEE Photon. Technol. Lett.*, vol. 25, no. 15, pp. 1408–1411, Aug. 2013.
[12] G. Agrawal, *Fiber-Optic Communication Systems*, 3rd Ed. New York, NY, USA: Wiley, 2002.
[13] Y. Park, M. Scaffardi, L. Potì, and J. Azaña, "Simultaneous singleshot real-time measurement of the instantaneous frequency and phase profiles of wavelength-division-multiplexed signals," *Opt. Exp.*, vol. 18, no. 6, pp. 6220–6229, Mar. 2010.
[14] M. Li and J. P. Yao, "Multichannel arbitrary-order photonic temporal differentiator for wavelength-division-multiplexed signal processing using a single fiber Bragg grating," *J. Lightw. Technol.*, vol. 29, no. 17, pp. 2506–2511, Sep. 2011.
[15] H. Yun, W. Shi, Y. Wang, L. Chrostowski, and N A. F. Jaeger, "2×2 adiabatic 3-dB coupler on silicon-on-insulator rib waveguides," *Proc. SPIE Photon. North*, vol. 8915, p. 89150V, May 2013.
[16] W. Bogaerts, R. Baets, P. Dumon, V. Wiaux, S. Beckx, D. Taillaert, B. Luyssaert, J. V. Campenhout, P. Bienstman, and D. V. Thourhout, "Nanophotonic waveguides in silicon-on-insulator fabricated with CMOS technology," *J. Lightw. Technol.*, vol. 23, no. 1, pp. 401–412, Jan. 2005.
[17] W. Bogaerts and S. K. Selvaraja, "Compact single-mode silicon hybrid rib/strip waveguide with adiabatic bends," *IEEE Photon. J.*, vol. 3, no. 3, pp. 422–432, Jun. 2011.
[18] W. Zhang, J. Zhang, and J. P. Yao, "Largely chirped microwave waveform generation using a silicon-based on-chip optical spectral shaper," in *Proc. MWP*, Sapporo, Japan, Oct. 2014, pp. 20–23.
[19] W. Bogaerts, "Silicon microring resonators," *Laser Photon. Rev.*, vol. 6, no. 1, pp. 47–73, Sep. 2012.
[20] Y. Zhang, S. Yang, A. E.-J. Lim, G.-Q. Lo, C. Galland, T. Baehr-Jones, and M. Hochberg, "A compact and low loss Y-junction for submicron silicon waveguide," *Opt. Exp.*, vol. 21, no. 1, pp. 1310–1316, Jan. 2013.
[21] Q. Chang, Q. Li, Z. Zhang, M. Qiu, T. Ye, and Y. Su, "A tunable broadband photonic RF phase shifter based on a silicon microring resonator," *IEEE Photon. Technol. Lett.*, vol. 21, no. 1, pp. 60–62, Jan. 2009.
[22] L.-W. Luo, G. Wiederhecker, K. Preston, and M. Lipson, "Power insensitive silicon microring resonators," *Opt. Lett.*, vol. 37, no. 4, pp. 590–592, Feb. 2012.
[23] W. H. P. Pernice, C. Schuck, M. Li, and H. X. Tang "Carrier and thermal dynamics of silicon photonic resonators at cryogenic temperatures," *Opt. Exp.*, vol. 19, no. 4, pp. 3290–3296, Feb. 2011.
[24] M. Li, L. Shao, J. Albert, and J. P. Yao, "Continuously tunable photonic fractional temporal differentiator based on a tilted fiber Bragg grating," *IEEE Photon. Technol. Lett.*, vol. 23, no. 4, pp. 251–253, Feb. 2011.

Weifeng Zhang (S'12) received the B.Eng. degree in electronic science and technology from Xi'an Jiaotong University, Xi'an, China, in 2008, and the M.A.Sc. degree in electrical engineering from the Politecnico di Torino, Torino, Italy, in 2011. He is currently working toward the Ph.D. degree at the Microwave Photonics Research Laboratory, School of Electrical Engineering and Computer Science, University of Ottawa, Ottawa, ON, Canada.

His current research interests include silicon photonics and its applications in microwave photonics.

Weilin Liu (S'10) received the B.Eng. degree in electronic information engineering from the University of Science and Technology of China, Hefei, China, in 2009, and the M.A.Sc. degree in electrical and computer engineering from the School of Electrical Engineering and Computer Science, University of Ottawa, Ottawa, ON, Canada, in 2011. He is currently working toward the Ph.D. degree at the Microwave Photonics Research Laboratory, School of Electrical Engineering and Computer Science, University of Ottawa, Ottawa, ON, Canada.

His research interests include microwave/terahertz generation, optical signal processing, fiber Bragg gratings, and their applications in microwave photonic systems.

Wangzhe Li (S'08) received the B.E. degree in electronic science and technology from Xi'an Jiaotong University, Xi'an, China, in 2004, the M.Sc. degree in optoelectronic and electronic science from Tsinghua University, Beijing, China, in 2007, and the Ph.D. degree in electrical engineering from the University of Ottawa, Ottawa, ON, Canada, in 2013.

He is currently a Postdoctoral Researcher with the Microwave Photonics Research Laboratory, School of Electrical Engineering and Computer Science, University of Ottawa. His current research interests include photonic generation of microwave and terahertz signals.

Dr. Li received the 2011 IEEE Microwave Theory and Techniques Society Graduate Fellowship and the 2011 IEEE Photonics Society Graduate Fellowship.

Hiva Shahoei (S'09) received the B.Sc. degree in electrical engineering from Tabriz University, Tabriz, Iran, in 2005, the M.Sc. degree in electrical engineering from Tehran Polytechnic University, Tehran, Iran, in 2008, and the Ph.D. degree in electrical engineering from the University of Ottawa, Ottawa, ON, Canada, in 2014.

Her current research interests include photonic processing of microwave signals, and slow and fast light and the applications in microwave photonics.

Dr. Shahoei received the 2012 IEEE Photonics Society Graduate Fellowship and the 2013 SPIE Graduate Scholarship.

Jianping Yao (M'99–SM'01–F'12) received the Ph.D. degree in electrical engineering from the Université de Toulon, Toulon, France, in December 1997.

He joined the School of Electrical and Electronic Engineering, Nanyang Technological University, Singapore, as an Assistant Professor in 1998. In December 2001, he joined the School of Electrical Engineering and Computer Science, University of Ottawa, Ottawa, ON, Canada, as an Assistant Professor, where he became an Associate Professor in 2003, and a Full Professor in 2006. He was appointed as the University Research Chair in Microwave Photonics in 2007. From July 2007 to June 2010, he was the Director of the Ottawa-Carleton Institute for Electrical and Computer Engineering. He was reappointed as the Director of the Ottawa-Carleton Institute for Electrical and Computer Engineering in 2013. He is currently a Professor and the University Research Chair in the School of Electrical Engineering and Computer Science, University of Ottawa. He has published more than 460 papers, including more than 260 papers in peer-reviewed journals and 200 papers in conference proceedings.

Prof. Yao was a Guest Editor for the Focus Issue on Microwave Photonics in *Optics Express* in 2013 and a Feature Issue on Microwave Photonics in *Photonics Research* in 2014. He is currently a Topical Editor for *Optics Letters*, and serves on the Editorial Board of the IEEE TRANSACTIONS ON MICROWAVE THEORY AND TECHNIQUES, *Optics Communications*, and *China Science Bulletin*. He is the Chair of numerous international conferences, symposia, and workshops, including the Vice-Technical Program Committee (TPC), the Chair of the IEEE Microwave Photonics Conference in 2007, the TPC Cochair of the Asia-Pacific Microwave Photonics Conference in 2009 and 2010, the TPC Chair of the high-speed and broadband wireless technologies subcommittee of the IEEE Radio Wireless Symposium in 2009–2012, the TPC Chair of the microwave photonics subcommittee of the IEEE Photonics Society Annual Meeting in 2009, the TPC Chair of the IEEE Microwave Photonics Conference in 2010, the General Cochair of the IEEE Microwave Photonics Conference in 2011, the TPC Cochair of the IEEE Microwave Photonics Conference in 2014, and the General Cochair of the IEEE the 2005 International Creative Research Award at the University of Ottawa, and the 2007 George S. Glinski Award for Excellence in Research. He was selected to receive an Inaugural OSA Outstanding Reviewer Award in 2012. He is an IEEE MTT-S Distinguished Microwave Lecturer for 2013–2015. He is also a registered Professional Engineer of Ontario. He is a Fellow of the Optical Society of America and the Canadian Academy of Engineering.